Decoupling Environmental Complexity: Direct Analysis in Sonar Performance Space

Jonas Halse Rygh[1] and Karl Thomas Hjelmervik[2]

[1]Norwegian Defence Research Establishment, Nedre vei 8, 3183 Horten, Norway
[2]University of South-Eastern Norway, Raveien 215, 3184 Borre, Norway

Contact author: J. H Rygh, Norwegian Defence Research Establishment, Nedre vei 8, 3183 Horten, Norway, e-mail: jonas-halse.rygh@ffi.no

Abstract: *The impact of environmental variability on sonar performance variability is crucial to understanding how to effectively manage sonar resources. Complexities arise due to the fact that it is the interplay between different environmental parameters that determine the sonar performance. It may not only be the sound speed profile, but also the bottom depth and wind speed. Consequently, there is need for an algorithm that can capture the combined effects of all included environmental parameters. We propose a method that uses empirical orthogonal functions and clustering on computed signal excesseses, in sonar performance space. This bypasses all environmental parameters altogether. The resulting clusters are then analysed and compared with the clusters one would get by only focusing on one environmental parameter, the sound speed profile in our case.*

Keywords: *Sonar performance modelling, Environment, Sonar operation planning aids.*

1. INTRODUCTION

Sonar performance modeling is crucial for planning sonar operations. Environmental data—such as bathymetry, sediment types, and oceanographic conditions—inform acoustic propagation models that estimate transmission loss and, for active sonar, expected reverberation levels [1]. The sonar equation allows the estimation of the signal excess, a parameter commonly used for the planning and execution of sonar missions [2].

In UACE 2023 [3] we proposed a method of organising the sonar environment into clusters of similar sound speed profiles, and further estimating the sonar performance based on representative sound speed profiles for each cluster. While this method is fast and programmatically simple, it fails to encompass other environmental parameters, such as bottom depths, sediment types, and ambient noise levels. For instance, two identical Munk profiles [4] with different bottom depths would be placed in the same cluster if a naive clustering algorithm on sound speed alone was used. In reality these two situations lead to fundamentally different sonar performance; one with convergence zones and one without depending on the bottom depths.

We propose an alternative method that bypasses all environmental parameters by compressing and clustering a pre-computed subset of signal excesses (or other 2D measures). This method captures the combined effects of the supplied environmental parameters, which can be arbitrarily many, at the cost of a significant increase in the computation time.

Here we apply the method on an area around the Vøring Plateau [5], with environmental data from Gebco [6] and Copernicus Marine Services [7].

2. METHOD

We select (lat, lon) in the extent $[\text{lat}_0, \text{lat}_1, \text{lon}_0, \text{lon}_1]$ such that the distance along any point is approximately Δ, which results in N points. The resulting grid is thus not uniform, but adjusted such that points near the poles are sampled less. Then we compute the signal excess for each point, using the acoustic model Lybin [8], with predefined sonar settings and environmental parameters using the supplied environmental data. The method is currently limited to range-independent environmental settings.

The signal excesses are then cropped to a selected depth interval $(z_{\text{min}}, z_{\text{max}})$, due to both numerical constraints (arrays must have the same dimensionality) and to limit the method to consider relevant depths (which should be determined by the application). The cropped signal excesses are then flattened to a vector, with dimensions $N_d = N_z \times N_r$, where N_z and N_r are the depth and range dimensionalities, respectively. The remaining EOF-analysis and clustering then follows the steps of [3]. We then form the matrix of signal excess vectors

$$\mathbf{S} = \begin{pmatrix} \vec{s}_1 & \vec{s}_2 & \dots & \vec{s}_N \end{pmatrix}^T, \tag{1}$$

where $\vec{s}_i$ is the flattened signal excess vector for $(\text{lat}_i, \text{lon}_i)$. We furthermore define the matrix

$$\mathbf{G} = \frac{\mathbf{S}_{\text{linear}} - \mu\left(\mathbf{S}_{\text{linear}}\right)}{\sigma\left(\mathbf{S}_{\text{linear}}\right)}, \tag{2}$$

where $\mu(x)$ and $\sigma(x)$ is the average and standard deviation of the signal excess matrix in linear scale along the N dimension with resulting dimensionality N_d. Next we use Empirical orthogonal function (EOF) analysis [9] and calculate the covariance matrix $\mathbf{X} = \mathbf{G}^T\mathbf{G}$, with

rank($\mathbf{X}$) = min(N, N_d). For a given N_d, we must there for at least have $N \geq N_d$ samples. The EOFs are the eigenvectors $\vec{u}$ of the covariance matrix

$$\mathbf{X}\vec{u} = \lambda\vec{u}, \tag{3}$$

and the EOF coefficients are given by

$$c_{ij} = \vec{g}_i \cdot \vec{u}_j, \tag{4}$$

where i runs over all N, and j runs over a subset of $N_{\text{pca}} < N_d$. The N_{pca} is selected such that most of the variance is contained in the reduced dataset, often set to a certain threshold. It is worth mentioning that this step may be crucial, as clustering algorithms struggle with large vector sizes. In our case, $N_d = N_z \times N_r$ can be quite large. This was not an isse in [3] since the dimensionality was of order $N_{\text{model-z}}$, where $N_{\text{model-z}}$ was the number of depths in the ocean model data. Lastly, a clustering algorithm, in our case K-means [10] is used on the coefficient matrix c_{ij}, with a predefined number of clusters.

3. DATA

The area of interest is given by the extent $[67°\text{N}, 70°\text{N}, 5°\text{W}, 5°\text{E}]$, which covers an area of about $A \approx 136,000\,\text{km}^2$. We gather bathymetry data from Gebco, and temperature and salinity profiles from MET [11] (compiled from Copernicus Marine Service) at time 14 September 2024, 20:00. Figure 1 presents the environmental parameters of the area.

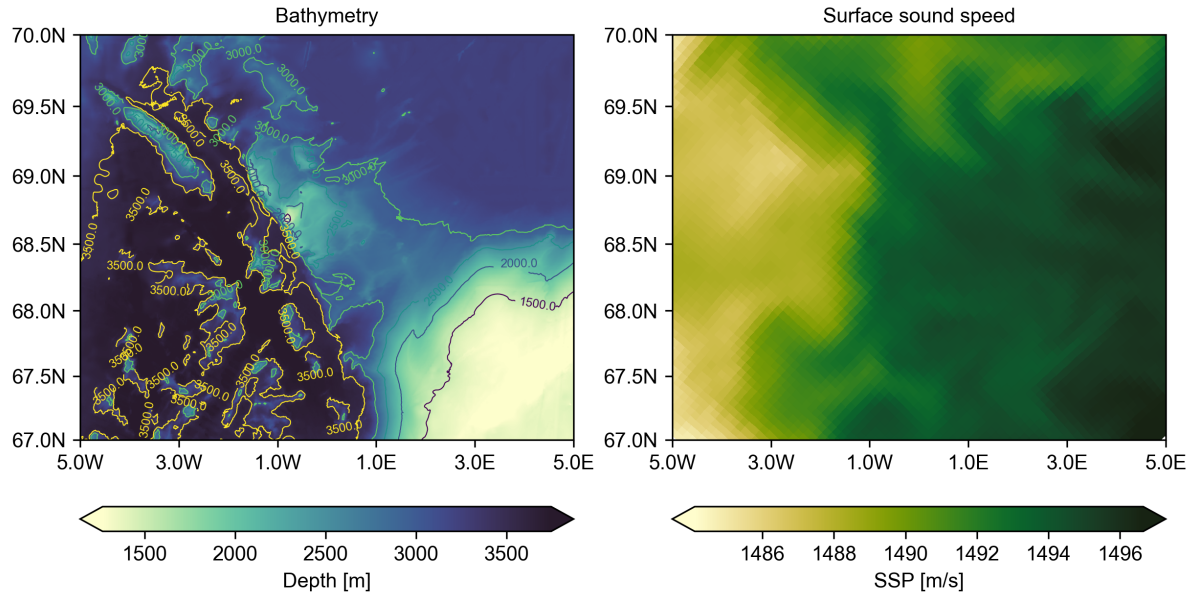

Figure 1: Plot of bathymetry data (left) and surface sound speed profile (right).

This area contains the Vøring plateau, which is seen in the bottom right corner, with bottom depths ranging from $1500\,\text{m}$ to $3500\,\text{m}$. The surface sound speed shows a variation of $10\,\text{m/s}$, from $\simeq 1486\,\text{m/s}$ in the west to $\simeq 1496\,\text{m/s}$ in the east. The reason for choosing this area is that it may or may not allow convergence zones.

4. RESULTS

The grid of latitudes and longitudes was generated using a spacing of $\Delta = 4.5\,\text{km}$, resulting in $N = 6791$ points. The depth interval was chosen to be $z_{\text{min}} = 0\,\text{m}$ and $z_{\text{max}} = 400\,\text{m}$, which results in a flattened dimensionality of $N_d = N_z \times N_r = 40 \times 140 = 5600 < N$, using $\Delta z = 10\,\text{m}$ and $\Delta r = 500\,\text{m}$ with a maximum range of $70\,\text{km}$. The transducer settings were for a generic long range sonar placed at depth $z = 50\,\text{m}$. The signal excesses were computed in 30 minutes, using a laptop computer.

The principal components were extracted from the averaged flattened signal excesses, using the PCA module from scikit-learn [12], using 320 components, chosen such that the explained variance was at 90%. The number of clusters were then visually determined to be $N_{\text{clusters}} = 7$, by observing when additional clusters were deemed negligible in size. The resulting clusters are shown in figure 3 and compared to the clusters from the method used in [3].

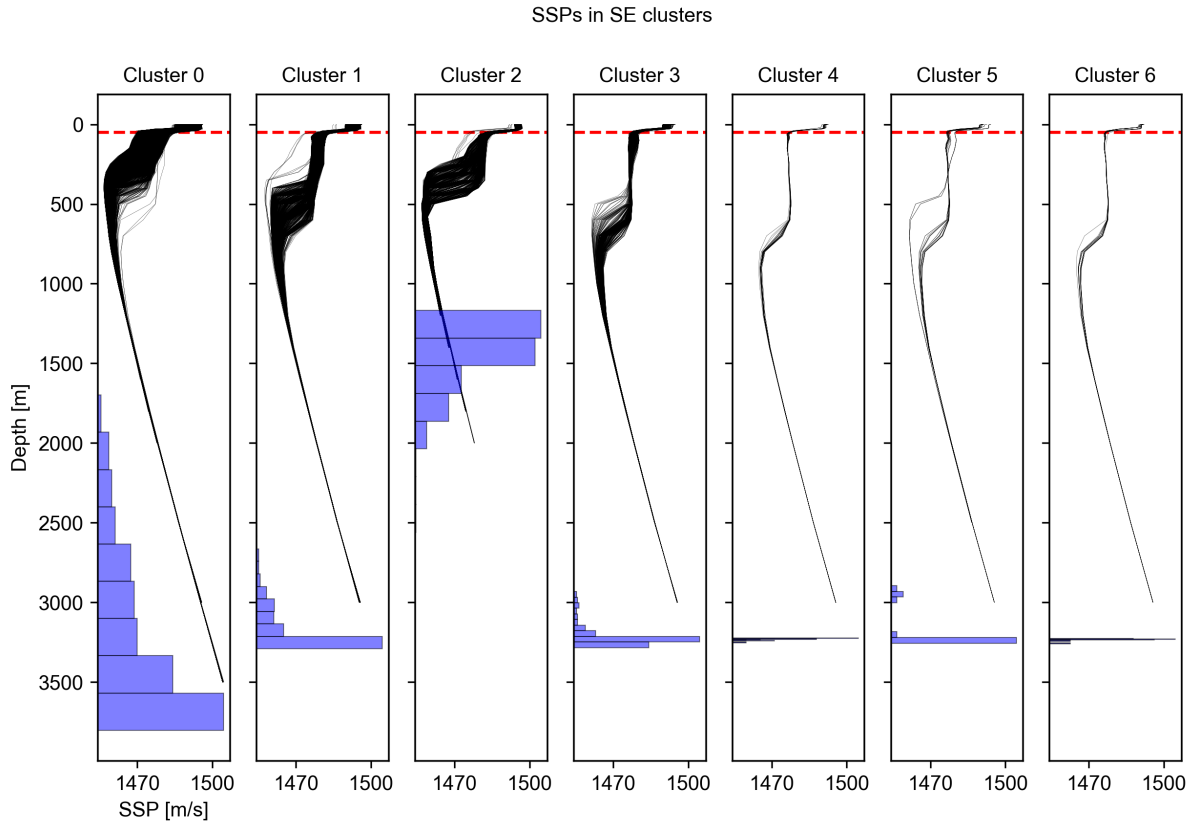

Figure 2: Sound speed profiles and bottom depth distributions for each cluster

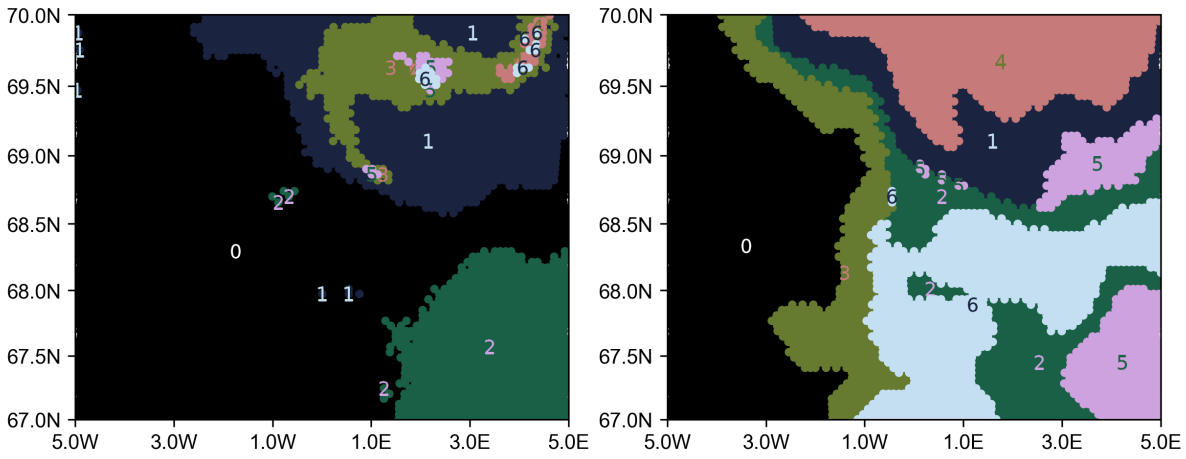

Figure 3: Clusters obtained using current method (left) and clusters obtained using the method in [3] (right)

Figure 4 shows the average and the 90th percentile (based on distances from cluster centroid) of the signal excess for each cluster, denoted by $\langle n \rangle$ and δn.

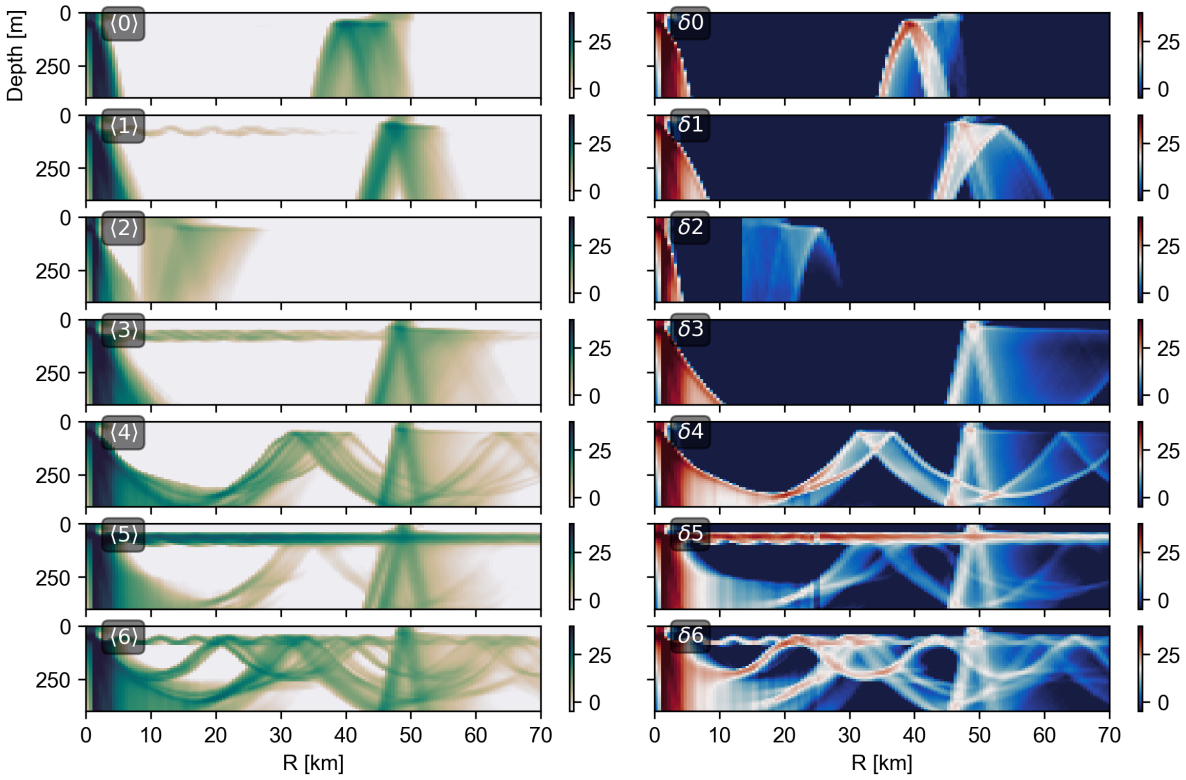

Figure 4: Average (left) and 90th percentile (right) of the signal excesses for each cluster, shown in logarithmic scale.

5. DISCUSSION

Consider figure 3, cluster 0 from both methods resemble each other to about 1°W, where the 0 cluster obtained from the proposed method continues eastward in a narrow passage between

cluster 1 and 2. Comparing with figure 2 we see that the overlapping area is very deep ($>$ $3000\,\mathrm{m}$) and contains sound speed surface values that are in the lower range of the surface values. We also observe that the clusters obtained from only considering sound speed profiles seem to capture areas with large gradients in surface sound speed values, and not bottom depths.

The most important result is found in the South-Easternmost area, where the bathymetry is around $1500\,\mathrm{m}$. The current method puts this area into one cluster, namely cluster 2. This cluster is not repeated elsewhere (except around $(69°\mathrm{N}, 1°\mathrm{W})$ where the depth is also around $1500\,\mathrm{m}$). This means that the cluster mostly contains shallow sound speed profiles and bottom depths ($1500\,\mathrm{m}$). Comparing this to the clusters found using the former method, we observe that the corresponding clusters, $2'$ and $5'$ (n' denotes clusters using the other method) contain sound speed profiles that are both shallow and deep ($3000\,\mathrm{m}$).

Now consider figure 4. We observe that the signal excess plots mainly describe two different situations: convergence zones in clusters $n_{\mathrm{cz}} \in \{0, 1, 3, 4, 5, 6\}$ and bottom reflections in clusters $n_{\mathrm{br}} \in \{2\}$. We also see that the 90th percentile and the average are almost similar for each cluster, which suggests that the average is representative for individual signal excesses in the covered area. The exception is for clusters 1 and 2, where some of the profiles contain a channel. They are expected to be allocated to a separate cluster, but this has not been achieved even by manipulating the number of clusters. Therefore, more work is to be done on this issue. However, the current method is an improvement since the former method results in single clusters containing both convergence zones and bottom reflections, which would be a poor representation of the sonar performance for an area. Thus, the current method can supply decision makers with maps that account for convergence zones.

From figure 4 we also observe differences within clusters describing the same situation. In n_{cz}, we see that the clusters $(3, 5, 6)$ have a variety of sound speed channels and are geographically close to each other; see figure 2. Cluster 4 is barely visible, but is located in the North-Easternmost area, in-between cluster 6, and almost contains a sound speed channel. Clusters $n_{\mathrm{cz}} = 0$ and $n_{\mathrm{cz}} = 1$ have pure convergence zones without sound speed channels. The convergence zone is also located at different ranges for different clusters, *e.g.* $40\,\mathrm{km}$ for cluster 0 and around $50\,\mathrm{km}$ for cluster 1. This is expected, as cluster 0 contains deeper depths $(3000\,\mathrm{m})$, allowing steeper angles to complete the loop before hitting the bottom.

The method seems successful in creating clusters that are physically relevant. Although this method seems to work as intended, there are currently several challenges. Firstly, the clusters are valid for only one set of sonar parameters. This may be fine for hull-mounted sonars, where the depth parameter is constant, but may be non-trivial for variable depth sonars. Secondly, the current method relies on range-independent environmental parameters. There are currently no obvious way of implementing range-dependent environmental parameters into a clustering algorithm. Finally, the new approach is significantly slower than the method described in [3].

6. SUMMARY

A clustering algorithm for geographical mapping of sonar performance was implemented and it's performance compared to an existing algorithm [3]. The new clustering approach decouples environmental complexities by clustering directly in sonar performance space. The sonar performance was estimated using the acoustic model Lybin [2] with input from both realistic oceanographic and bathymetric data. The resulting clusters were shown to be physically relevant and could be divided into clusters influenced by convergence zones and bottom reflection. Lastly, the method demonstrated that correct predictions of sonar performance relies on

the interplay between several different environmental parameters, and that naively focusing on one alone is not sufficient.

REFERENCES

[1] J. M. Hovem, *Marine Acoustics - The Physics of Sound in Underwater Environments*. Peninsula Publishing, 2012.

[2] E. M. Bøhler, P. Østenstad, and K. T. Hjelmervik, "A Monte Carlo approach for capturing the uncertainty in sonar performance modelling," p. 8.

[3] J. H. Rygh, K. T. Hjelmervik, and T. Jenserud, "Sonar performance modelling for clustered watermasses," in *Proceedings of the Underwater Acoustics Conference and Exhibition*, (Kalamata, Greece), pp. 693–700, Institute of Applied and Computational Mathematics (I.A.C.M.), Foundation for Research and Technology – Hellas (FORTH), June 2023.

[4] W. H. Munk, "Sound channel in an exponentially stratified ocean, with application to sofar," *The Journal of the Acoustical Society of America*, vol. 55, pp. 220–226, 02 1974.

[5] D. Myer, S. Constable, and K. Key, "Magnetotelluric evidence for layered mafic intrusions beneath the vøring and exmouth rifted margins," *Physics of the Earth and Planetary Interiors*, vol. 220, p. 1–10, 07 2013.

[6] G. B. C. G. 2023, "The gebco_2023 grid - a continuous terrain model of the global oceans and land.," Apr 2023.

[7] Copernicus Marine Service, "Copernicus marine environment monitoring service (cmems)." `https://marine.copernicus.eu`. Accessed: 2024-04-01.

[8] E. Dombestein and T. Jenserud, "Improving Underwater Surveillance: LYBIN Sonar performance Prediction," in *MAST Americas 2010*, (Washington DC, USA), 2010.

[9] K. T. Hjelmervik and K. Hjelmervik, "Improved estimation of oceanographic climatology using empirical orthogonal functions and clustering," in *2013 MTS/IEEE OCEANS - Bergen*, pp. 1–5, June 2013.

[10] P. Virtanen, R. Gommers, T. E. Oliphant, M. Haberland, T. Reddy, D. Cournapeau, E. Burovski, P. Peterson, W. Weckesser, J. Bright, S. J. van der Walt, M. Brett, J. Wilson, K. J. Millman, N. Mayorov, A. R. J. Nelson, E. Jones, R. Kern, E. Larson, C. J. Carey, İ. Polat, Y. Feng, E. W. Moore, J. VanderPlas, D. Laxalde, J. Perktold, R. Cimrman, I. Henriksen, E. A. Quintero, C. R. Harris, A. M. Archibald, A. H. Ribeiro, F. Pedregosa, P. van Mulbregt, and SciPy 1.0 Contributors, "SciPy 1.0: Fundamental Algorithms for Scientific Computing in Python," *Nature Methods*, vol. 17, pp. 261–272, 2020.

[11] Norwegian Meteorological Institute, "Arctic ocean physics analysis and forecast, 6.25 km 1-hourly frequency." `https://thredds.met.no/thredds/catalog/fou-hi/topaz5-arc-1hr_files/catalog.html`.

[12] F. Pedregosa, G. Varoquaux, A. Gramfort, V. Michel, B. Thirion, O. Grisel, M. Blondel, P. Prettenhofer, R. Weiss, V. Dubourg, J. Vanderplas, A. Passos, D. Cournapeau,

M. Brucher, M. Perrot, and E. Duchesnay, “Scikit-learn: Machine learning in Python,” *Journal of Machine Learning Research*, vol. 12, pp. 2825–2830, 2011.